Received: 15 February 2022 | Revised: 19 June 2022 | Accepted: 26 July 2022

DOI: 10.1002/term.3344

WILEY

RESEARCH ARTICLE

Studies on oxygen availability and the creation of natural and artificial oxygen gradients in gelatin-methacryloyl hydrogel 3D cell culture

Carola Schmitz | Iliyana Pepelanova | Christian Ude | Antonina Lavrentieva

Institute of Technical Chemistry, Gottfried Wilhelm Leibniz University Hannover, Hannover, Germany

Correspondence
Antonina Lavrentieva, Institute of Technical Chemistry, Gottfried Wilhelm Leibniz University Hannover, Hannover, Germany.
Email: lavrentieva@iftc.uni-hannover.de

Funding information
German Research Foundation, Grant/Award Number: 398007461 488; Ministry of Science and Culture of Lower Saxony

Abstract

Three-dimensional (3D) cultivation platforms allow the creation of cell models, which more closely resemble in vivo-like cell behavior. Therefore, 3D cell culture platforms have started to replace conventional two-dimensional (2D) cultivation techniques in many fields. Besides the advantages of 3D culture, there are also some challenges: cultivation in 3D often results in an inhomogeneous microenvironment and therefore unique cultivation conditions for each cell inside the construct. As a result, the analysis and precise control over the singular cell state is limited in 3D. In this work, we address these challenges by exploring ways to monitor oxygen concentrations in gelatin methacryloyl (GelMA) 3D hydrogel culture at the cellular level using hypoxia reporter cells and deep within the construct using a non-invasive optical oxygen sensing spot. We could show that the appearance of oxygen limitations is more prominent in softer GelMA-hydrogels, which enable better cell spreading. Beyond demonstrating novel or space-resolved techniques of visualizing oxygen availability in hydrogel constructs, we also describe a method to create a stable and controlled oxygen gradient throughout the construct using a 3D printed flow-through chamber.

KEYWORDS
3D cell culture, AD-MSCs, hydrogels, hypoxia reporter cells, hypoxia sensor, oxygen concentration measurements

Three-dimensional (3D) cell culture holds a promise for many technological advancements ranging from tissue engineering to cell biology studies. The higher complexity of the 3D model allows the in vitro reconstruction of a situation resembling in-vivo conditions, complete with intercellular communication, cell-matrix interactions and the existence of biochemical and mechanical gradients (Petrenko et al., 2017). Complex 3D cultivation methods could thus support the development of artificial tissues whether for transplantation purposes or for the creation of physiologically relevant in vitro models. In scaffold-based 3D culture techniques, cells are cultivated on or in scaffold materials, which support a 3D organization of the construct. The search for suitable scaffold materials is challenging: materials do not only have to be biocompatible, but also be preferably biodegradable, enabling cells to replace the non-endogenous material with their own extracellular matrix over time (Qiu et al., 2019).

From this perspective, hydrogels, especially those derived from the extracellular matrix exhibiting signaling and attachment motifs, have shown very promising results so far (González-Díaz & Varghese, 2016). The hydrogel polymers form insoluble networks that contain high amounts of water by chemical or physical cross-linking, resulting in an aqueous environment similar to the one existing in many tissues in vivo. The advantages of 3D cell cultivation

in hydrogels have been widely discussed in the scientific literature, including providing a specific spatial cell morphology (Tibbitt & Anseth, 2009), higher local concentrations of secreted signaling molecules, as well as the presence of various gradients similar to in vivo tissues (Griffith & Swartz, 2006). In contrast to other 3D cultivation methods, for example, spheroid cultures, the use of hydrogels enables the researcher to gain control over the mechanical properties of the cell's surrounding area. Previous studies have shown that cell fate (Engler et al., 2006), adherence (Yeung et al., 2005) and proliferation (Peyton et al., 2006) depend on the biomechanical features of the applied scaffold material. For example, stem cells sense the stiffness of their surrounding hydrogel matrix by mechanotransduction (Trappmann & Chen, 2013) and differentiate according to the information provided by the artificial extracellular matrix. Different 3D culture studies confirm that osteogenic differentiation is preferred in more rigid hydrogels, while adipogenic differentiation is increased in softer hydrogels (Huebsch et al., 2010; Parekh et al., 2011). Mechanobiology studies cell-material interactions and is a broad field with a complex interplay of many factors, which have been discussed in-depth in the following publications (Mehrabi et al., 2018; Yang et al., 2017).

The higher complexity of 3D cell cultivation systems does not only come with advantages, but exhibits its own sets of challenges: The analysis of cellular behavior in 3D is much more complex than established assays in two dimensions (2D). While we assume that cells in a 2D system experience an unnatural but homogenous microenvironment, cells in 3D have different ranges of nutrient availability, waste disposal and gas supply (Edmondson et al., 2014). Assays accessing cell viability indirectly are not capable of reflecting the individual situation that cells experience in their specific 3D loci. However, other established methods such as cell staining and cross-sections through the construct can still be applied for cell state and proliferation analysis in 3D (Chai et al., 2016; Kirsch et al., 2021).

The analysis of the cells' microenvironment is of interest as well. For the purpose of mimicking a natural microenvironment, the control, or at least the analysis of oxygen availability in 3D cell culture constructs is invaluable to put cellular behavior in the right context. The importance of oxygen for cellular processes cannot be overstated as O_2 availability controls the cell's energy metabolism (erobic respiration or anaerobic glycolysis), protein expression and differentiation potential (Samal et al., 2021). For example, severe hypoxia in the early embryonic state preserves the pluripotency of eukaryotic stem cells (Prasad et al., 2009). In mesenchymal stem cells (MSCs), the effect of hypoxia on chondrogenic, osteogenic and adipogenic differentiation has been extensively studied (Samal et al., 2021). Therefore, oxygen supply is a crucial parameter for 3D cultivation methods, with cells ideally being cultivated under oxygen levels similar to their specific in vivo niche to ensure an *in vivo*-like cell response. Exact oxygen control in 2D and 3D cultivation systems is also important because oxygen is often the limiting nutrient not only because of limited diffusion, but also due to the poor solubility in aqueous media, especially by higher temperatures, which are used for cell cultivations (Martin & Vermette, 2005).

Several oxygen measurement methods have been applied for 3D hydrogel constructs so far. For example, Boyce et al. created a hydrogel with an oxygen gradient and visualized the respective O_2 concentrations with an oxygen sensing film, which was accessed by microscopy (Boyce et al., 2019). This 2D visualization of oxygen is certainly helpful, but does not allow the monitoring of O_2 distribution along the *Z*-axis. A method applied by Figueiredo et al. and Prante et al. allows the analysis of oxygen concentration along the *Z*-axis. These groups used a sensor positioning system equipped with microsensors to penetrate into the hydrogel, which enables an oxygen concentration evaluation in different depths of the 3D construct (Figueiredo et al., 2018; Prante et al., 2018). Even an automated system for high-throughput testing based on this setup was developed (Eggert et al., 2021). Unfortunately, this method is invasive and many holes must be poked into the material to represent valid oxygen profiles all over the gel. This may change hydrogel features over longer measurement periods. Another recently developed technique relies on oxygen sensing microbeads: These are embedded in the scaffold material and can be evaluated by microscopy. Since the movement of the beads is restricted by the hydrogel, the researcher can access the same point of the gel again and again over different cultivation time periods. Lesher-Pérez et al. used this method to model the oxygen availability in cell-loaded hydrogels (Lesher-Pérez et al., 2017). The application of specific measurement points allows more flexibility, but is also limited to the initial localization of the microbeads. Non-invasive oxygen measurements in sterile cultivation setups have also been performed with the help of oxygen sensor spots. These were originally developed for glass reactors, cultivation bags or spinners (Lavrentieva et al., 2010), but are also suitable for transparent hydrogel-based 3D culture constructs as shown in our study.

An alternative approach to monitor oxygen distribution in 3D cell culture was developed by our lab. We created hypoxia reporter MSCs, which express the fluorescent UnaG protein at certain low levels of available oxygen (Schmitz et al., 2020). We could demonstrate that modified MSCs quantitatively react to the O_2 concentration (fluorescence in direct relation to the O_2 concentration). The expression of the reporter protein is under control of hypoxia-response elements, which are triggered by the cell's key transcription factor for low oxygen concentrations: hypoxia inducible factor 1α (HIF-1α). This constitutively expressed protein gets constantly degraded when oxygen is available. If oxygen deprivation occurs, HIF-1α enters the nucleus and triggers cascades of pathways for cellular adaptations (Kumar & Choi, 2015).

In this study, we are the first to adapt the use of oxygen sensor spots, which are traditionally used in the monitoring of microbial fermentations, to the monitoring of oxygen concentration in hydrogels. While this is great, it still shows oxygen concentration at a particular level, not throughout the whole construct. In addition, we used reporter cells to visualize the oxygen as cells experience it in their specific positions in the hydrogel. We could show that a natural oxygen gradient develops in some hydrogels. It could be of interest to create an artificial and stable, reproducible oxygen gradient. For this purpose, we designed a 3D printed flow chamber.

1 | MATERIALS AND METHODS

1.1 | GelMA-hydrogel preparation and polymerization

Gelatin-methacryloyl (GelMA) was synthesized and characterized (degree of functionalization [DoF] of 42% as determined with the Ninhydrin assay) as previously described (Pepelanova et al., 2018) and dissolved in phosphate-buffered saline (PBS) at 3.5%; 4%; 4.5% (w/v) (Loessner et al., 2016). Precise temperature control was performed prior to the polymerization process. The hydrogel was warmed up to 33°C and 0.2% (w/v) photoinitiator (Irgacure 2959; Sigma Aldrich) was added. If applicable, cells were suspended by soft pipetting. During the entire preparation process 33°C was applied for the hydrogel solution. Prior to polymerization, the hydrogel was cooled down to 25°C for 3 min with the aid of a warming plate. Polymerization was performed in a UV irradiation system (Bio-Link®; Vilber Lourmat) at 1.4 J/cm^2.

1.2 | Rheological measurements

Rheological measurements were performed using a MCR 302 Modular Rheometer (Anton Paar) equipped with a plate-plate geometry (⌀ 20 mm). To determine the material stiffness, the storage and loss moduli were recorded by a time sweep oscillatory test (strain amplitude 1%, frequency of 1 Hz) with a gap size of 0.6 mm resulting in a sample volume of 200 µL. The test was performed for a total of 10 min, with the material exposed to UV-light for 5 min and examined in the dark for an additional 5 min. The solutions were stored at 33°C and cooled down to 25°C by the rheometer 3 min prior measurement.

1.3 | Experimental setup for non-invasive oxygen measurement

A sensor spot approach was chosen for non-invasive oxygen measurements in hydrogels. Optical signals were analyzed with a multichannel oxygen meter (Oxy-4 mini; PreSens GmbH). Polymer optical fibers (POF) (2.0 mm core, PreSens GmbH) were installed in the incubator (CO_2-Incubator C16, Labotect). An inset with 4 channels fitting a 24-well plate was screwed on the incubator shelf, guaranteeing a stable central positioning of the light transmitters under the well (Figure 1a). Inside the actual wells, a silicone ring was glued as a mold for hydrogel polymerization. A 3D printed holder (Figure 1b) was used to control the height of the incorporated oxygen sensor spot (SP-PSt3-NAU; d = 3 mm; PreSens GmbH) and introduced in the hydrogel prior to polymerization. For system calibration, the sensor spot was inserted into the holder, positioned in the respective silicone ring and 1 ml PBS was added. When the measured oxygen signal in the incubator (37°C, 5% CO_2) was stable, calibration was set as 100% O_2 saturation. Zero point calibration was performed by saturated Na_2SO_3 solution in PBS.

1.4 | Re-oxygenation of hydrogels to determine oxygen permeability for different polymer/precursor concentrations

GelMA-hydrogels of 100 µL volume were polymerized as described above and oxygen was withdrawn by addition of 500 µL PBS with Na_2SO_3 (0.25% w/v) and $CoCl_2$ (0.2 mM). After Na_2SO_3 consumption, oxygen diffusion into the respective hydrogels was measured for 30 h. Curves for the respective hydrogel re-oxygenation were compared to the re-oxygenation of 500 µL PBS with Na_2SO_3 (0.25% w/v) and $CoCl_2$ (0.2 mM) without hydrogel.

1.5 | 3D printing of the holder and flow chamber and print purification

The 3D models (sensor spot holder and flow chamber) were designed by Autodesk Inventor Professional 2019 (Autodesk GmbH), transformed into a .stl-format and 3D printed with the help of MultiJet 3D printing (MJP 2500 Plus, 3D Systems Inc.). M2-RCL was used as the printing material, M2-SUP was applied as support material (3D Systems Inc.). For purification, the objects were cleaned from the support material in water steam and any leftovers were dissolved in paraffin oil at 65°C (Carl Roth GmbH und Co. KG). The oil was removed by anionic surfactant water at 65°C and ultrasonic bath (Siller et al., 2020). Prior to EtOH disinfection, all objects were cleaned with ddH_2O. The designs were adapted to fit commercially available products: the holder fits a 3 mm oxygen sensor spot (Figure 2a), the flow chamber was incorporated in a bigger petri dish (ø 94 mm, Greiner bio-one) to maintain sterility and adapted to a silicone hose (ID 2.6 mm) for oxygen supply.

1.6 | Cell culture

Hypoxia reporter cells (transduced hAD-MSCs) were previously created and characterized (Schmitz et al., 2020). Cells were expanded in α-minimum essential medium (α-MEM; Thermo Fisher Scientific) containing 1 g/L glucose, 2 mM l-glutamine, 10% human serum (CC-Pro), and 50 µg/ml gentamicin (Merck KGaA), harvested by accutase treatment (Merck KGaA). Cultivation was performed in the incubator at 37°C and 5% CO_2. Cells cultivated in 2D (T175 flasks, Sarstedt) were washed with PBS, detached from the flask by accutase (5 ml) for 5 min and centrifuged at 300 xg with additional cultivation media (5 ml). Cell number was determined by manual counting in a hemocytometer and the required cell number for hydrogel encapsulation was pelleted and consequently re-suspended in the non-polymerized hydrogel.

1.7 | Oxygen gradient generation in a flow chamber

Hydrogel and hypoxia reporter cells were prepared as described above. A hydrogel concentration of 4% GelMA with 3 mio cells/ml

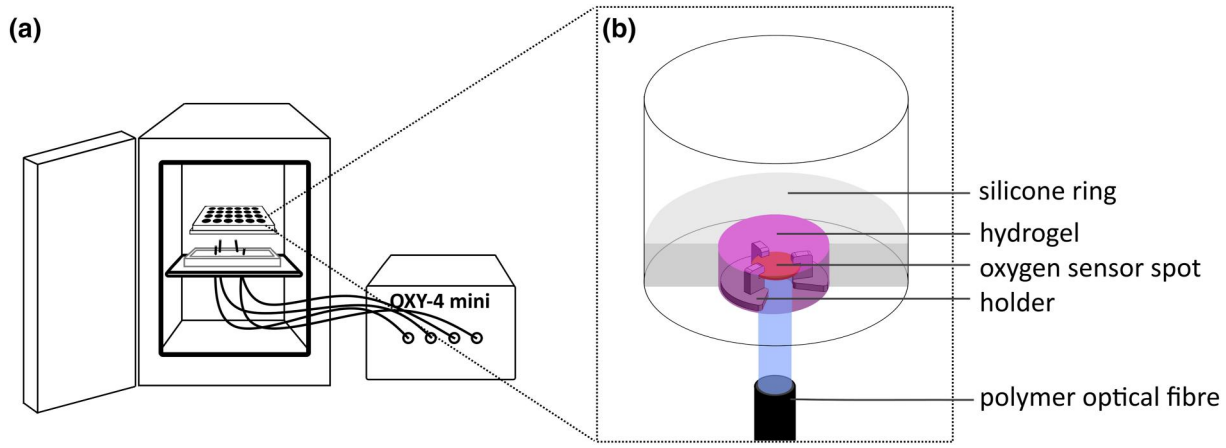

FIGURE 1 Experimental setup for non-invasive optical oxygen measurements in 3D hydrogel based constructs. (a) O_2-controllable incubator was equipped with an inset for POFs, which are positioned under the respective measurement wells. The POFs are let through the incubators' sealing to connect to the multi-channel oxygen meter. (b) The measurement wells (24-well plate) are equipped with a silicone mold, which centers the hydrogel. A 3D printed holder guarantees that the sensor spot is always at the same height. POF, polymer optical fibers [Colour figure can be viewed at wileyonlinelibrary.com]

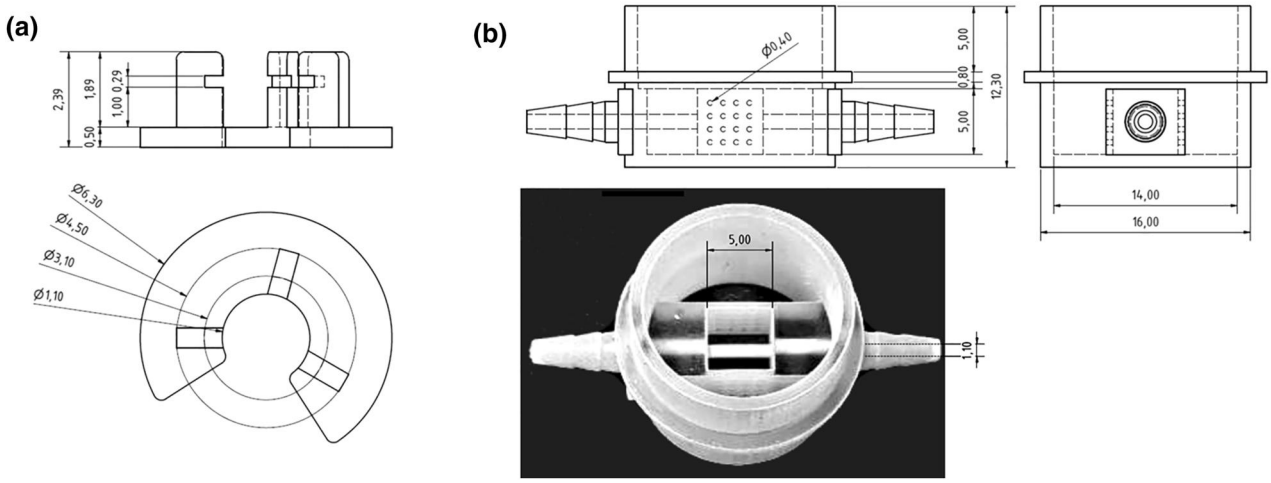

FIGURE 2 Dimensions of the 3D printed objects. (a) Oxygen sensor spot holder. (b) Flow chamber for oxygen gradient creation. Stl.-data files can be obtained from the supplementary material

was chosen and the polymerization process was performed directly in the flow chamber (Figure 2b). The flow chamber was attached to a silicone tubing (ID 2.6 mm), which was connected to a peristaltic pump (REGLO ICC, ISMATEC®) to supply the hydrogel with air (21% O_2) from outside of the incubator. The incubator O_2 concentration was set to 3.5%.

1.8 | Microscopy of hydrogel constructs

Hydrogel constructs had to be stabilized in order to cut them manually. For this purpose, the constructs were embedded in 2% agarose (Carl Roth). A razorblade (ISANA MEN, Rossmann GmbH) was used to cut out a slice at the middle of the construct. The slide obtained in this manner was again embedded in 2% agarose for imaging via Cytation®5 multimode imaging reader (BioTek® Instruments).

1.9 | Statistical analysis

The data is presented as mean value ± standard deviation of three measurements of each sample ($n = 3$). One-way ANOVA (MS Excel) was performed to determine the statistical significance of the measured values, defined as p-value of $^*p < 0.05$. Linear regression (S3) was performed with OriginLab.

2 | RESULTS

This work was conducted in order to offer easy and reliable methods for visualizing oxygen content and distribution in GelMA-hydrogels and other transparent polymers for 3D cell culture applications. The oxygen permeability of the GelMA-hydrogel was first characterized under cell-free conditions, by applying an optical non-invasive

oxygen sensor spots with the help of 3D printed holders for fixation. Additionally, hypoxia reporter cells were embedded in the construct, offering researchers visualization of oxygen concentration as experienced by the cell at a single cell level resolution throughout the whole global construct. The application of non-invasive oxygen measurement methods and hypoxia sensor cells in 3D enabled an online monitoring of in situ oxygen availability and a visualization of oxygen gradients (Figure S1).

2.1 | Oxygen permeability in GelMA-hydrogels with varying stiffness

The relation of hydrogel concentration and the permeability for O_2 was investigated as a factor for possible oxygen supply limitations. GelMA-hydrogels (3.5%; 4%; 4.5% w/v) without cells were equipped with an oxygen sensor spot. After oxygen withdrawal by Na_2SO_3, the oxygen influx (from ambient conditions in the incubator at appr. 18.6% O_2) in the hydrogel was observed over 30 h. GelMA-hydrogels of higher concentration/stiffness (4%; 4.5%) display a faster re-oxygenation compared to the less concentrated polymers (Figure S2). However, at the start of the measurement (0–2 h) the speed of re-oxygenation is almost similar for all hydrogel concentrations (Figure 3a).

For GelMA, the hydrogel stiffness relates linearly to the concentration of the hydrogel, which was measured by rheology, and evaluated by linear regression with the help of Origin data analysis software (OriginLab corporation) (Figure S3). In order to make sure that later results are comparable with cell loaded materials, the stiffness between cell-free and cell-loaded constructs was examined (Figure 3b). Cell encapsulation didn't influence material properties for all tested concentrations.

2.2 | Oxygen measurements and visualization of oxygen gradients in cell-loaded GelMA-hydrogels

The oxygen concentration of cell-loaded GelMA-hydrogels (5 mio cells/ml) with different concentrations/stiffness (3.5%: 100 Pa; 4%: 160 Pa; 4.5%: 245 Pa) was observed for a duration of 48 h (Figure 4a). The polymerization process of GelMA uses up all oxygen inside the hydrogel prior measurements. When the constructs are positioned in the incubator and oxygen measurements are commenced, a phase of re-oxygenations is visible (<30 min, Figure S4). At this point, cells are still adapting to their new environment until oxygen concentration reaches a peak and subsequently decreases due to metabolic oxygen consumption. Oxygen decrease is more pronounced in GelMA-hydrogels of lower precursor concentration (Figure 4b), although all hydrogels contain the same number of cells (5 mio/ml). Moreover, the oxygen concentration is not stable over time and seems to depend on the dynamic microenvironment. While GelMA-hydrogels of weaker stiffness (3.5%) remained at low oxygen content (<10% v/v) over 2 days, cells embedded in GelMA of 4.5% would experience an oxygen concentration of 30% at its lowest and oxygen levels would rise over the next day. Protracted measurements in GelMA of 4.5% confirmed that the oxygen concentration stays dynamic and decreases over the time span of a week (Figure S5).

Although online measurements in hydrogels are a useful tool to observe changes in oxygen during an ongoing experiment, they don't provide acess to the oxygen distribution throughout the construct. To visualize the hypoxia profile in 3D, a setup similar to the oxygen measurements experiments was choosen. For spatial visualization of hypoxia onset through the entire hydrogel constructs, we used previously created hypoxia reporter MSCs, which fluorescence signal was sensitive to different oxygen levels (mean fluorescence at 2.5% O_2—1.3×10^6 relative fluorescence units (RFU), at 5% O_2—1.0×10^6 RFU and at 7.5% O_2—0.4×10^6 RFU; Schmitz et al., 2020). Reporter MSCs were embedded in the GelMA-hydrogels without oxygen measurement equipment and cultivated for 48 h under ambient culture conditions. For microscopic access, a slice in the center of the hydrogel was cut out after 2 days. In a manner already observed during the oxygen concentration measurements, GelMA-hydrogels with lower stiffness exhibited stronger hypoxia reporter cell response in comparison to hydrogels of higher stiffness (Figure 5a). Hypoxia was also mostly detectable at the bottom center of the gels. The construct is supplied with oxygen by diffusion from the covering media and subsequently areas with the furthest diffusion distance show the strongest signal. For GelMA of 3.5% a clear gradient of the hypoxia signal could be visualized. Additionally, a change in the cells' morphology could be observed (Figure 5b) in GelMA of low stiffness. As stated in previous studies, less stiff materials enable cell spreading while stiffer hydrogels inhibit this behavior (Lavrentieva et al., 2020). The energy required for spreading and migration possibly causes an increase in oxygen consumption. Accordingly, the measured oxygen concentrations in constructs enabling cell spreading were lower than in hydrogels where cells mostly remain in their rounded shape. The resulting gradient in fluorescence serves as an overview for the researcher, helping evaluate at which depth and at what pattern oxygen limitations occur in such experimental setups. Additionally, GelMA of 3.5% undergoes a strong shift in its geometry due to cell traction forces, which leads to a denser gel construct, causing a higher cell concentration in this area and therefore a higher local oxygen consumption.

2.3 | Creation of oxygen gradients in hydrogels

As it was shown above, cultivation of cells in 3D hydrogel constructs can cause the appearance of natural oxygen gradients. Such gradients can however be of great interest if controllable gradient platforms could be created. For this purpose, a flow chamber was designed and 3D printed, which allows oxygen to diffuse radially from within the construct. Here, the oxygen concentration in the incubator overlay was set to 3.5% and the cell-loaded GelMA-hydrogel was penetrated by a capillary membrane, which supplied the construct with air (21% O_2) from outside of the incubator (Figure 6a). As a result, a radial gradient could be observed that shows that cells next to the membrane receive a high amount of oxygen while cells in the outer area of the hydrogel

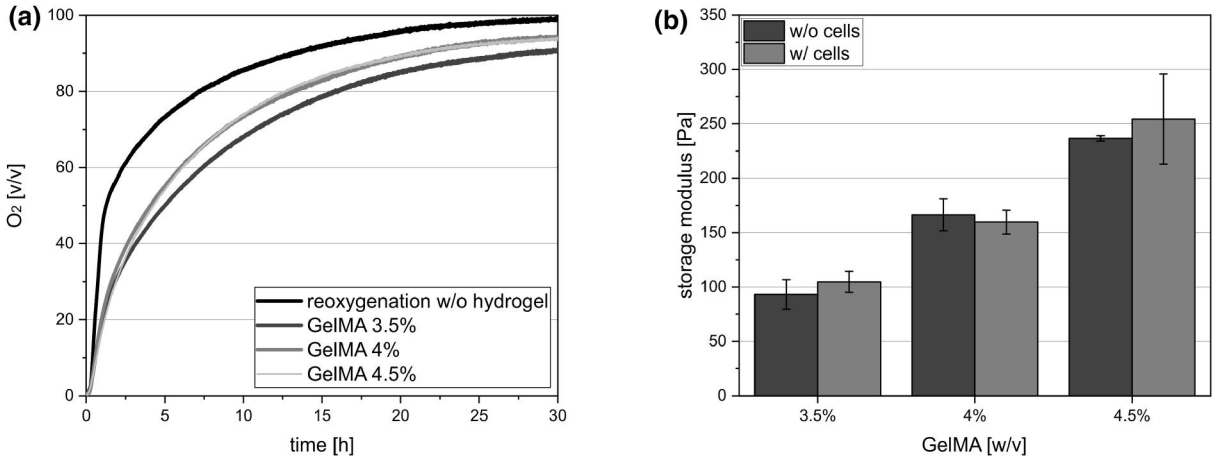

FIGURE 3 Properties of GelMA-hydrogels in terms of (a) oxygen permeability after oxygen depletion by Na_2SO_3 and subsequent re-oxygenation ($n = 3$) and (b) stiffness modulus in dependence of material concentration without and with cells (5 mio/ml) ($n = 3$). Analysis of variance (p-value < 0.05) showed no statistical differences between hydrogels with or without cells of similar GelMA concentration. GelMA, gelatin-methacryloyl

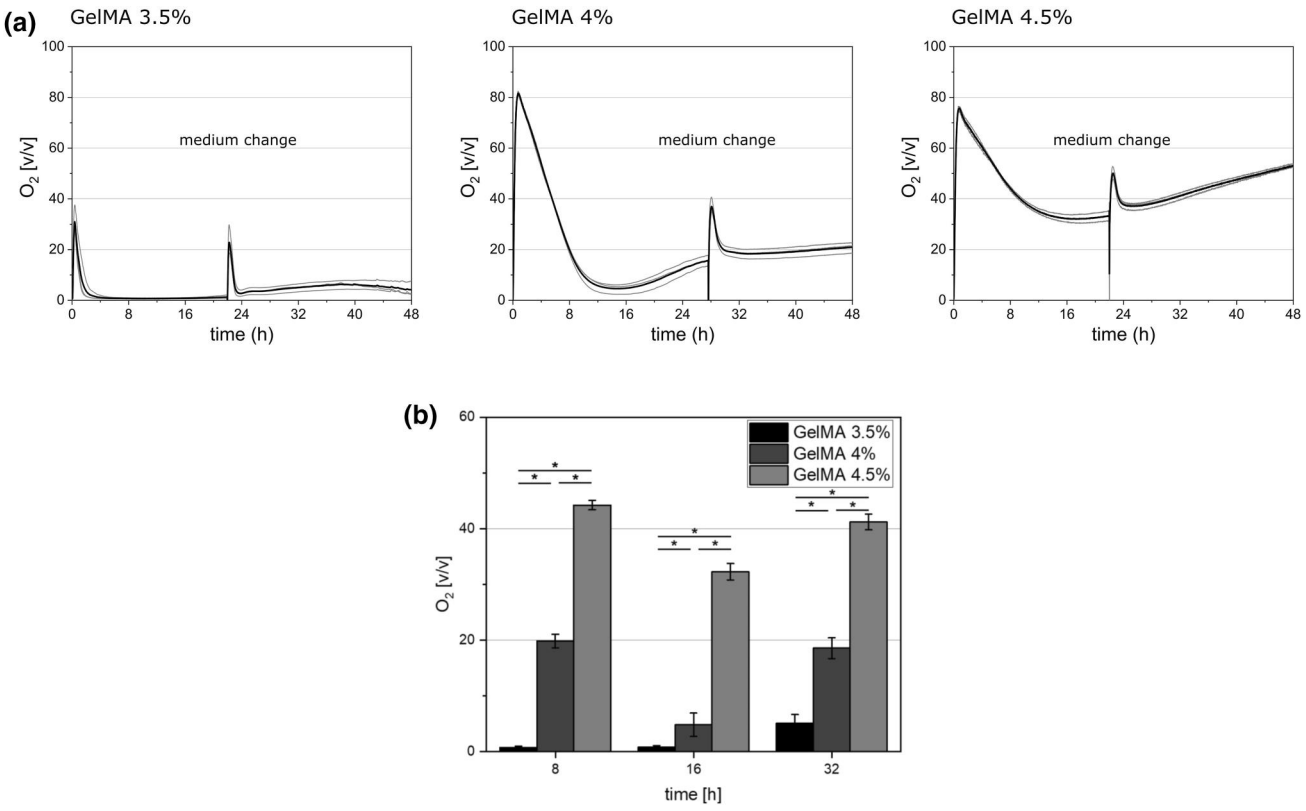

FIGURE 4 (a) Oxygen measurements in GelMA-hydrogels with 5 mio cells/ml of varying polymer concentration. Measurements were performed in three independent hydrogels (gray). The average output is represented in black. (b) Oxygen concentrations in cell-loaded GelMA-hydrogels (3.5%, 4%, 4.5%) after 8, 16, 32 h of cultivation ($n = 3$). Significance in O_2 measurements was analyzed by one-way ANOVA (*$p < 0.05$). GelMA, gelatin-methacryloyl

display a strong hypoxia signal due to the oxygen withdrawal through the incubator (Figure 6b). The flow-chamber approach allows the researcher to create an inhomogeneous environment with increased control of the oxygen availability. Desired hypoxia profiles can be generated by variations of the speed or pressure of the oxygen pump, the oxygen concentration in the incubator or the diameter of the capillary membrane.

3 | DISCUSSION

Commonly used methods to analyze 3D cell culture scaffold materials for their functionality are pore size, material stiffness, swelling ratio, their biocompatibility and their ability to promote cell differentiation. Along with finding optimal mechanical and biological properties of materials, the control of oxygen availability within 3D constructs

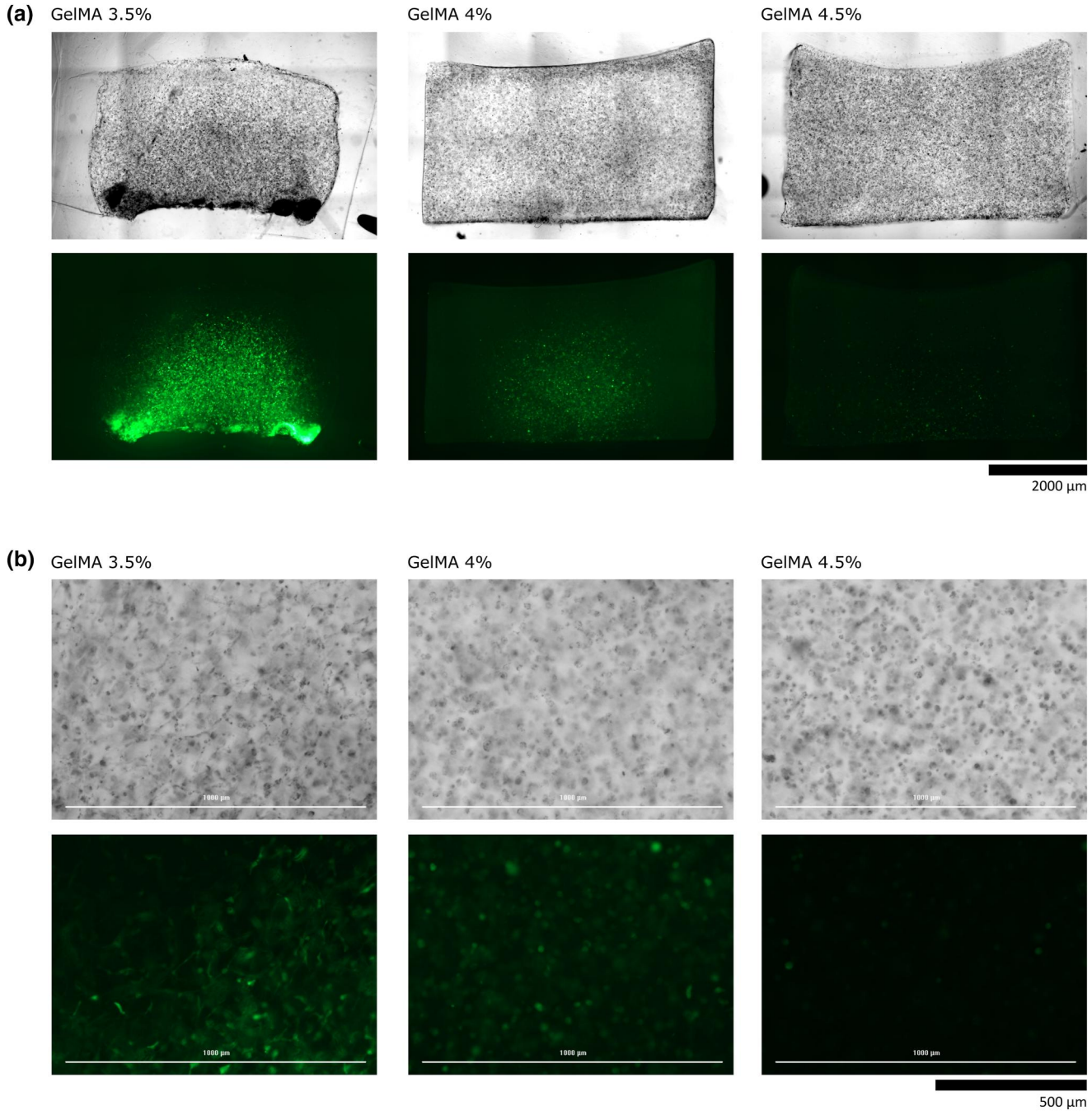

FIGURE 5 Cross-sections of GelMA-hydrogels (3.5%; 4%; 4.5% w/v) with 5 mio hypoxia reporters cells/ml embedded (48 h of incubation). (a) The whole cross-section is displayed, allowing a visualization of the naturally occurring oxygen gradients, which are present in GelMA of 3.5%, and barely visible for GelMA of 4.5%. (b) Close-up of the respective cross-sections. For GelMA of 3.5% cell spreading and hypoxia reporter cell output is clearly visible. For GelMA of 4.5% no cell spreading can be observed. GelMA, gelatin-methacryloyl [Colour figure can be viewed at wileyonlinelibrary.com]

remains a major challenge. This work aims to analyze the oxygen availability, to study the appearance of natural oxygen gradients, as well as to create artificially induced oxygen gradients in 3D cell culture constructs in dependence of the hydrogel's stiffness.

To investigate the influence of the hydrogel stiffness/concentration on oxygen diffusion, GelMA-hydrogels without cells were analyzed in terms of their oxygen permeability by re-oxygenation after oxygen withdrawal. Measurements with non-invasive oxygen sensor spots could show that for GelMA-hydrogels no direct relationship between oxygen diffusion and polymer concentration/hydrogel stiffness exists. At very low oxygen levels (<20% O_2), diffusion into the construct was equally fast for all concentrations, while oxygen diffusion in GelMA of 3.5% was slightly slower at high O_2 levels. The mesh size of such hydrogel-polymer networks is often made responsible for diffusion limitations, but the size of the oxygen molecule is much too small and should not be affected by steric

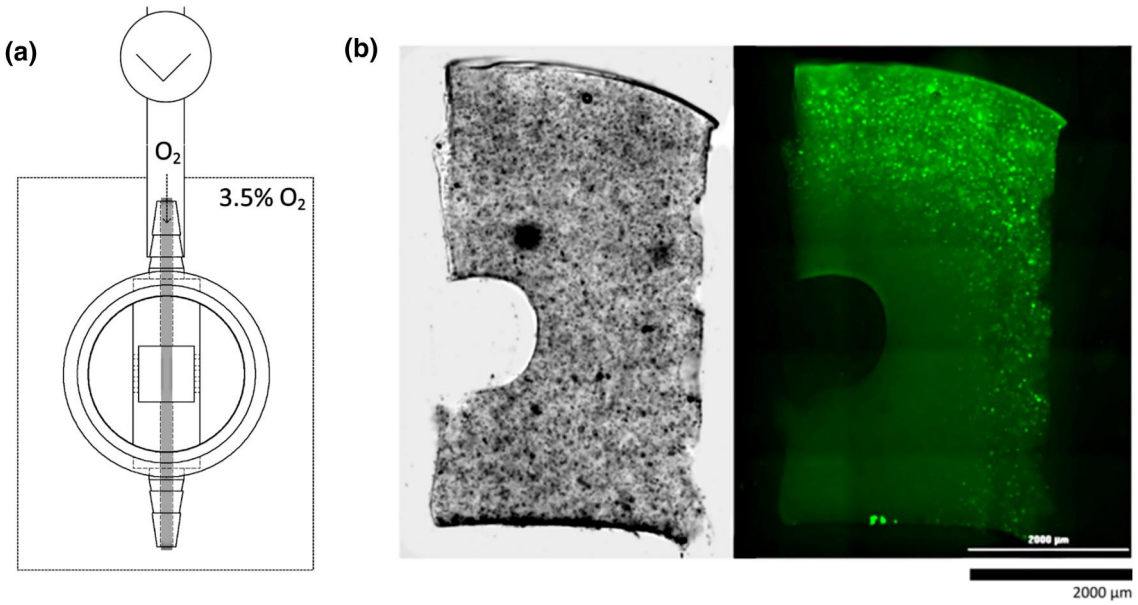

FIGURE 6 Generated oxygen gradient (a) created by a flow chamber, where a capillary membrane intervenes a cell loaded gelatin-methacryloyl-hydrogel (4%) with hypoxia reporter cells (3 mio cells/ml). A peristaltic pump supplies the membrane with air from outside of the incubation chamber, while the O_2 concentration in the incubator is lowered to 3.5% O_2. (b) A radial gradient of hypoxia signal can be observed when the hydrogel is cut at the center, displaying the area where oxygen limitations occur and hypoxia cell response is activated [Colour figure can be viewed at wileyonlinelibrary.com]

hindrances. Similar experiments were performed by Figueiredo et al., who calculated the half-life for hydrogel re-oxygenation for silated-hydroxypropylmethylcellulose hydrogels without cells (Figueiredo et al., 2018). The research group also did not observe direct influence of the polymer concentration on the permeability of oxygen.

To ensure that the mechanical properties (in terms of hydrogel stiffness) remain the same when cells are embedded in the GelMA-hydrogel, rheological measurements were performed. No influence of the embedded MSCs on GelMA-hydrogel stiffness was observed directly after hydrogel polymerization. But nevertheless, cell-dependent hydrogel alterations remain of importance for experiments performed over multiple days. For cell-loaded GelMA-hydrogel constructs, a decrease of the hydrogel's stiffness was previously reported at cultivation durations >24 h (Martinez-Garcia et al., 2021), whereas hydrogels of higher polymer concentration would retain their mechanical properties for multiple days. The authors stated that the hydrogel undergoes constant scaffold remodeling by the embedded cells, which is faster at low hydrogel stiffness.

On-line oxygen measurements help evaluate the local O_2 concentration without altering the scaffold material and are also applicable in cell-loaded hydrogel constructs. In this study, strong oxygen deprivation was shown in cell-loaded GelMA-hydrogels of weaker stiffness (GelMA 3.5% after 16 h: 1% O_2), while oxygen availability in stiffer hydrogels (GelMA 4.5% after 16 h: 23% O_2) remained comparably high. Since the re-oxygenation of hydrogels of varying stiffness without cells did not display a relevant difference in terms of oxygen permeability of the hydrogels, the cellular activity and metabolism (as shown by cell spreading in GelMA 3.5%) must be responsible for low oxygen content in hydrogels of lower mechanical stiffness. These measurements displayed the oxygen content at the center of the construct, where the sensor spot was located. However, oxygen gradients are generated through oxygen diffusion limitations throughout the 3D construct, which cannot be monitored by oxygen sensor spots. Here, hypoxia reporter cells were used to visualize the final oxygen distribution in a 3D construct to reveal the spatial profile of oxygen availability. These cells show where oxygen diffusion limitation occurs and give quantitative information of the degree of oxygen deprivation. In a manner similar to the experiments with the sensor spot, the highest reporter output was seen in GelMA 3.5% hydrogels. In this case, the strongest hypoxia signal was detected at the center and the bottom of the construct, since oxygen diffuses into the construct from the surrounding media above. A similar pattern was found in GelMA 4% hydrogels, but with a much weaker signal, while cells embedded in the stiffest applied material (GelMA 4.5%) would show almost no signal, indicating hypoxia is almost not present. Presented measurements were performed under ambient oxygen concentrations in the incubator and reflect changes in local oxygen tensions caused solely by diffusion and consumption in the GelMA-construct. If oxygen concentration in the incubator will be decreased and constructs will be cultivated in hypoxic conditions, in situ situation will be different. Cell behavior and oxygen measurements in hydrogel constructs cultivated in hypoxia must be studied in further experiments.

GelMA-hydrogels which enabled better cell spreading demonstrated an increased hypoxia signal compared to constructs of similar cell number which enable cell spreading to a lesser degree (Figure 5). Therefore, the actual oxygen uptake does not only vary among different cell types (Wagner et al., 2011) but is additionally influenced by cellular activity as direct result from surrounding hydrogel composition/stiffness. Previously, other groups created mathematical

models to calculate oxygen gradients in 3D cell cultures, often calculating oxygen consumption activity by using the Michaelis-Menten-kinetics (Lesher-Pérez et al., 2017; McReynolds et al., 2017). Also much more complex formulas, which include additional parameters (e.g., unequal cell distribution or hypoxia-mediated cell death) can be applied, but they need to be fitted precisely to the chosen cultivation method and the constant remodeling of the scaffold material is rarely considered (Mavris & Hansen, 2021). Whether mathematical models can forecast oxygen distribution over a longer period of time with a constant remodeling of the scaffold material and changing cellular behavior (spreading, proliferation, differentiation) is questionable. Therefore, oxygen measurements and reporter cell application hold valuable and easily accessible information for anyone performing 3D cell culture.

The existence of oxygen gradients in 3D cell culture settings should be carefully considered as anoxia does not only cause cell death, but HIF influences the overall cell state and behavior (Koh & Powis, 2012). Variations in the experimental setup could influence the degree of hypoxia and therefore the outcomes of studies. For 3D models, platforms which allow increased control over the oxygen supply could lead to more realistic 3D cultivation platforms and prevent unwanted cell death through anoxia. The flow chamber presented in this study allows the creation of controllable and variable radial oxygen gradients in 3D hydrogel constructs. The use of a flow chamber for gradient generation combined with hypoxia reporter cells for visualization allows precise setting of experimental parameters for various research questions. Implementation of controlled oxygen gradients in 3D hydrogel-based constructs can be a useful tool for both, recreating physiological oxygen gradients in poorly vascularized tissues (e.g., cartilage) for Tissue Engineering, as well as for recapitulation of pathological conditions in tumors and wounds. Such gradients can help to create better in vitro disease models and functional tissues.

4 | CONCLUSION

The oxygen permeability of scaffold materials for 3D cell culture experiments plays an important role in the generation of oxygen gradients. Scaffold materials that stimulate cell behavior leading to higher energy demand, display steeper oxygen gradients as the oxygen consumption of the cells increases. In addition to the monitoring of the formation of spontaneous gradients in 3D constructs, artificial oxygen gradients can be recreated in vitro. The 3D flow chamber developed in this work can serve as helpful tool to create such gradients.

AUTHOR CONTRIBUTIONS

Carola Schmitz designed and performed the experiments. Iliyana Pepelanova provided the GelMA-hydrogel and supervised its use. Christian Ude helped to design the non-invasive oxygen measurement and gave advice related to the performed oxygen measurement. Antonina Lavrentieva provided the hypoxia reporter cells and research environment as well as expert knowledge about 3D cell cultivation. Carola Schmitz, Iliyana Pepelanova, and Antonina Lavrentieva wrote the article.

ACKNOWLEDGMENTS

This study was funded by the German Research Foundation (DFG Project 398007461 488 "3D Dual-Gradient Systems for Functional Cell Screening" and "BiomolecularSensor Platform for Elucidating Hypoxic Signatures in 2D and 3D in vitro culture Systems"). This work was also supported by the Ministry of Science and Culture (MWK) of Lower Saxony, Germany through the SMART BIOTECS alliance between the Technische Universität Braunschweig and the Leibniz Universität Hannover. Moreover, we would like to thank Dr. Janina Bahnemann and Steffen Winkler, who provided the 3D printing setup as well as Vsevolod V. Belousov and Ekaterina Potekhina for providing sensor plasmids.

CONFLICT OF INTEREST

The authors have no conflicts of interest to declare.

DATA AVAILABILITY STATEMENT

The data that support the findings of this study are available from the corresponding author upon reasonable request.

REFERENCES

Boyce, M. W., Simke, W. C., Kenney, R. M., & Lockett, M. R. (2019). Generating linear oxygen gradients across 3D cell cultures with block-layered oxygen controlled chips (BLOCCs). *Analytical Methods*, *12*(1), 18–24. https://doi.org/10.1039/c9ay01690b

Chai, Y. W., Lee, E. H., Gubbe, J. D., & Brekke, J. H. (2016). 3D cell culture in a self-assembled nanofiber environment. *PLoS One*, *11*(9), e0162853. https://doi.org/10.1371/journal.pone.0162853

Edmondson, R., Broglie, J. J., Adcock, A. F., & Yang, L. (2014). Three-dimensional cell culture systems and their applications in drug discovery and cell-based biosensors. *Assay Drug Development Technologies*, *12*(4), 207–218. https://doi.org/10.1089/adt.2014.573

Eggert, S., Gutbrod, M. S., Liebsch, G., Meier, R., Meinert, C., & Hutmacher, D. W. (2021). Automated 3D microphysiometry facilitates high-content and highly reproducible oxygen measurements within 3D cell culture models. *ACS Sensors*, *6*(3), 1248–1260. https://doi.org/10.1021/acssensors.0c02551

Engler, A. J., Sen, S., Sweeney, H. L., & Discher, D. E. (2006). Matrix elasticity directs stem cell lineage specification. *Cell*, *126*(4), 677–689. https://doi.org/10.1016/J.CELL.2006.06.044

Figueiredo, L., Pace, R., D'Arros, C., Rethore, G., Guicheux, J., Le Visage, C., & Weiss, P. (2018). Assessing glucose and oxygen diffusion in hydrogels for the rational design of 3D stem cell scaffolds in regenerative medicine. *Journal of Tissue Engineering Regenerative Medicine*, *12*(5), 1238–1246. https://doi.org/10.1002/term.2656

González-Díaz, E. C., & Varghese, S. (2016). Hydrogels as extracellular matrix analogs. *Gels*, *2*(3), 20. https://doi.org/10.3390/gels2030020

Griffith, L. G., & Swartz, M. A. (2006). Capturing complex 3D tissue physiology in vitro. *Nature Reviews Molecular Cell Biology*, *7*(3), 211–224. https://doi.org/10.1038/nrm1858

Huebsch, N., Arany, P. R., Mao, A. S., Shvartsman, D., Ali, O. A., Bencherif, S. A., Rivera-Feliciano, J., & Mooney, D. J. (2010). Harnessing traction-mediated manipulation of the cell/matrix interface to control stem-cell fate. *Nature Materials*, *9*(6), 518–526. https://doi.org/10.1038/nmat2732

Kirsch, M., Rach, J., Handke, W., Seltsam, A., Pepelanova, I., StrauB, S., Vogt, P., Scheper, T., & Lavrentieva, A. (2021). Comparative analysis of mesenchymal stem cell cultivation in fetal calf serum, human serum, and platelet lysate in 2D and 3D systems. *Frontiers in Bioengineering and Biotechnology*, *8*. https://doi.org/10.3389/fbioe.2020.598389

Koh, M. Y., & Powis, G. (2012). Passing the baton: The HIF switch. *Trends in Biochemical Sciences*, *37*(9), 364–372. https://doi.org/10.1016/j.tibs.2012.06.004

Kumar, H., & Choi, D. K. (2015). Hypoxia inducible factor pathway and physiological adaptation: A cell survival pathway? *Mediators of Inflammation*, *2015*, 1–11. https://doi.org/10.1155/2015/584758

Lavrentieva, A., Fleischhammer, T., Enders, A., Pirmahboub, H., Bahnemann, J., & Pepelanova, I. (2020). Fabrication of stiffness gradients of GelMA hydrogels using a 3D printed micromixer. *Macromolecular Bioscience*, *20*(7), 2000107. https://doi.org/10.1002/mabi.202000107

Lavrentieva, A., Majore, I., Kasper, C., & Hass, R. (2010). Effects of hypoxic culture conditions on umbilical cord-derived human mesenchymal stem cells. *Cell Communication and Signaling*, *8*, 1–9. https://doi.org/10.1186/1478-811X-8-18

Lesher-Pérez, S. C., Kim, G. A., Kuo, Ch., Leung, B. M., Mong, S., Kojima, T., Moraes, C., Thouless, M. D., Luker, G. D., & Takayama, S. (2017). Dispersible oxygen microsensors map oxygen gradients in three-dimensional cell cultures. *Biomater. Sci.*, *5*(10), 2106–2113. https://doi.org/10.1039/c7bm00119c

Loessner, D., Meinert, C., Kaemmerer, E., Martine, L. C., Yue, K., Levett, P. A., Klein, T. J., Melchels, F. P. W., Khademhosseini, A., & Hutmacher, D. W. (2016). Functionalization, preparation and use of cell-laden gelatin methacryloyl-based hydrogels as modular tissue culture platforms. *Nature Protocols*, *11*(4), 727–746. https://doi.org/10.1038/nprot.2016.037

Martin, Y., & Vermette, P. (2005). Bioreactors for tissue mass culture: Design, characterization, and recent advances. *Biomaterials*, *26*(35), 7481–7503. https://doi.org/10.1016/j.biomaterials.2005.05.057

Martinez-Garcia, F. D., Valk, M. M., Sharma, P. K., Burgess, J. K., & Harmsen, M. C. (2021). Adipose tissue-derived stromal cells alter the mechanical stability and viscoelastic properties of gelatine methacryloyl hydrogels. *International Journal of Molecular Sciences*, *22*(18), 10153. https://doi.org/10.3390/IJMS221810153

Mavris, S. M., & Hansen, L. M. (2021). Optimization of oxygen delivery within hydrogels. *Journal of Biomechanical Engineering*, *143*(10). https://doi.org/10.1115/1.4051119

McReynolds, J., Wen, Y., Li, X., Guan, J., & Jin, S. (2017). Modeling spatial distribution of oxygen in 3d culture of islet beta-cells. *Biotechnology Progress*, *33*(1), 221–228. https://doi.org/10.1002/btpr.2395

Mehrabi, M., Amini, F., & Mehrabi, S. (2018). Active role of the necrotic zone in desensitization of hypoxic macrophages and regulation of CSC-fate: A hypothesis. *Frontiers Oncology*, *8*(JUN), 1–9. https://doi.org/10.3389/fonc.2018.00235

Parekh, S. H., Chatterjee, K., Lin-Gibson, S., Moore, N. M., Cicerone, M. T., Young, M. F., & Simon, C. G. (2011). Modulus-driven differentiation of marrow stromal cells in 3D scaffolds that is independent of myosin-based cytoskeletal tension. *Biomaterials*, *32*(9), 2256–2264. https://doi.org/10.1016/J.BIOMATERIALS.2010.11.065

Pepelanova, I., Kruppa, K., Scheper, T., & Lavrentieva, A. (2018). Gelatin-methacryloyl (GelMA) hydrogels with defined degree of functionalization as a versatile toolkit for 3D cell culture and extrusion bioprinting. *Bioengineering*, *5*(3), 55. https://doi.org/10.3390/bioengineering5030055

Petrenko, Y., Syková, E., & Kubinová, Š. (2017). The therapeutic potential of three-dimensional multipotent mesenchymal stromal cell spheroids. *Stem Cell Research and Therapy*, *8*(1), 1–9. https://doi.org/10.1186/s13287-017-0558-6

Peyton, S. R., Raub, C. B., Keschrumrus, V. P., & Putnam, A. J. (2006). The use of poly(ethylene glycol) hydrogels to investigate the impact of ECM chemistry and mechanics on smooth muscle cells. *Biomaterials*, *27*(28), 4881–4893. https://doi.org/10.1016/J.BIOMATERIALS.2006.05.012

Prante, M., Ude, C., Große, M., Raddatz, L., Krings, U., John, G., Belkin, S., & Scheper, T. (2018). A portable biosensor for 2, 4-dinitrotoluene vapors. *Sensors (Switzerland)*, *18*(12), 4247. https://doi.org/10.3390/s18124247

Prasad, S. M., Czepiel, M., Cetinkaya, C., Smigielska, K., Weli, S. C., Lysdahl, H., Gabrielsen, A., Petersen, K., Ehlers, N., Fink, T., Minger, S. L., & Zachar, V. (2009). Continuous hypoxic culturing maintains activation of Notch and allows long-term propagation of human embryonic stem cells without spontaneous differentiation. *Cell Proliferation*, *42*(1), 63–74. https://doi.org/10.1111/j.1365-2184.2008.00571.x

Qiu, Y. L., Chen, X., Hou, Y., Hou, Y., Tian, S., Chen, Y., Yu, L., Nie, M., & Liu, X. (2019). Characterization of different biodegradable scaffolds in tissue engineering. *Molecular Medicine Reports*, *49*(5), 4043–4056. https://doi.org/10.3892/mmr.2019.10066

Samal, J. R. K., Rangasami, V. K., Samanta, S., Varghese, O. P., & Oommen, O. P. (2021). Discrepancies on the role of oxygen gradient and culture condition on mesenchymal stem cell fate. *Advanced Healthcare Materials*, *10*(6), 2002058. https://doi.org/10.1002/adhm.202002058

Schmitz, C., Pepelanova, I., Seliktar, D., Potekhina, E., Belousov, V. V., Scheper, T., & Lavrentieva, A. (2020). Live reporting for hypoxia: Hypoxia sensor–modified mesenchymal stem cells as in vitro reporters. *Biotechnology and Bioengineering*, *117*(2), 3265–3276. https://doi.org/10.1002/bit.27503

Siller, I. G., Enders, A., Gellermann, P., Winkler, S., Lavrentieva, A., Scheper, T., & Bahnemann, J. (2020). Characterization of a customized 3D-printed cell culture system using clear, translucent acrylate that enables optical online monitoring. *Biomedical Materials*, *15*(5), 055007. https://doi.org/10.1088/1748-605X/ab8e97

Tibbitt, M. W., & Anseth, K. S. (2009). Hydrogels as extracellular matrix mimics for 3D cell culture. *Biotechnology and Bioengineering*, *103*(4), 655–663. https://doi.org/10.1002/BIT.22361

Trappmann, B., & Chen, C. S. (2013). How cells sense extracellular matrix stiffness: A material's perspective. *Current Opinion in Biotechnology*, *24*(5), 948–953. https://doi.org/10.1016/J.COPBIO.2013.03.020

Wagner, B. A., Venkataraman, S., & Buettner, G. R. (2011). The rate of oxygen utilization by cells. *Free Radical Biology and Medicine*, *51*(3), 700–712. https://doi.org/10.1016/j.freeradbiomed.2011.05.024

Yang, Y., Wang, K., Gu, X., & Leong, K. W. (2017). Biophysical regulation of cell behavior—Cross talk between substrate stiffness and nanotopography. *Engineering*, *3*(1), 36–54. https://doi.org/10.1016/J.ENG.2017.01.014

Yeung, T., Georges, P. C., Flanagan, L. A., Marg, B., Ortiz, M., Funaki, M., Zahir, N., Ming, W., Weaver, V., & Janmey, P. A. (2005). Effects of substrate stiffness on cell morphology, cytoskeletal structure, and adhesion. *Cell Motillity and the Cytoskeleton*, *60*(1), 24–34. https://doi.org/10.1002/CM.20041

SUPPORTING INFORMATION

Additional supporting information can be found online in the Supporting Information section at the end of this article.

How to cite this article: Schmitz, C., Pepelanova, I., Ude, C., & Lavrentieva, A. (2022). Studies on oxygen availability and the creation of natural and artificial oxygen gradients in gelatin-methacryloyl hydrogel 3D cell culture. *Journal of Tissue Engineering and Regenerative Medicine*, *16*(11), 977–986. https://doi.org/10.1002/term.3344